Article

Development of TiC/ $Cr_{23}C_6$ Composite Coating on St 304 Substrate through TIG Process

Behzad Heidarshenas [1,*] and Ghulam Hussain [2]

[1] Department of Mechanical Engineering, Eastern Mediterranean University, Gazimagusa, North-Cyprus, via Mersin 10, Turkey
[2] GIK Institute of Engineering Sciences & Technology, Topi, KP, Pakistan, ghulam.hussain@giki.edu.pk
* Correspondence: behzad.shenas@emu.edu.tr

Abstract: The aim of this paper is to develop a composite coating on St 304 steel employing TIG process. Ti wire cored with graphite powder is used as the means of coating material. The process parameters are varied in order to develop coating with optimum characteristics (i.e., hardness and wear resistance). The microstructure of the coating is analyzed with SEM and XRD. It is found that both of the hardness and wear resistance increase as the current increases while both of these properties decrease as the travelling speed increases. It is found that the coated samples with composite layers have more hardness than the substrate and it could range up to 1100 HV being almost 4.5 times higher than the hardness of St 304. Likewise, the wear resistance of coating is observed to be 4.5 times higher than that of substrate. The high performance of coating, as revealed by microstructural analysis, is due to formation of TiC and $Cr_{23}C_6$ .The optimum conditions to produce the coating are proposed to be 120 A current and 3.17 mm/s travel speed.

Key Words: TIG process; Composite Coating; St 304; Hardness; Wear Resistance

---

1. Introduction

Steel is one of the widely used alloys. Every year million tons of these alloys are being produced in the world. It has a wide variety of applications ranging from kitchen appliances to heavy railways. High performance steel alloys are developed with good corrosion resistance, excellent ductility, high toughness, and high temperature oxidation and creep resistance [1-6].

Some of the steels tend to gall when they are brought into contact with other metallic materials, thus exhibiting poor wear resistance. Surface modification is one of the most important and effective industrial methods for improving wear properties of such steels. A number of methods have been applied to improve the surface properties including chemical and physical vapor deposition, ion implantation, and electron and laser beam [7-10]. The chemical and physical vapor deposition forms a thin layer on the surface, thus involving high production time. Whereas, electron beam and laser techniques produce concentrated heat which melts a rather thick coating layer on the substrate.

In the surface modification methods such as electron beam and laser in which a highly concentrated heat source is used, the wear resistance at high loads is maintained due to the production of a thick, adhesive and hard coating layer, so it is applicable where high load is involved[11-14]. However, electron beam and laser processes also have limitations such as need of vacuum chamber, and high equipment and production costs.

Recently, TIG (Tungsten Inert Gas) process has been employed as a cost effective alternative in surface modification technology. In this Method, a torch that provides high power density is traversed over the substrate surface and causes absorption of a large amount of energy in a short period of time and creates the melt/substrate interface which penetrates into the substrate in a short time. Because of temperature gradient between the surface layer and the substrate, the melt immediately freezes and a layer with metallurgical bond to the base metal is developed. Short time of process, saving in costs, energy, and material consumption besides high precision are the main advantages of this process in surface engineering[11].

Peer-reviewed version available at Coatings 2017, 7, , 80; doi:10.3390/coatings7060080

Baytoret et al. [15]employed TIG process to produce a wear resistant composite coating on the surface of 304 Steel. The SiC powder was mixed into the molten pool of steel to make the desired surface composite, leading to the hardness increase up to 6 times.

Both of metallic and ceramic powders can be utilized to form a composite onto a metallic substrate, and there are two ways to mix these powders into the substrate surface. Either by directly applying the powder onto the substrate or by using powder cored filler wires [16-22].

Metallic composites are amongst the most interesting new materials having qualified mechanical-tribological properties. In these developed materials, a non-metallic secondary phase in form of powder, fibers or Viskers is dispersed in a metallic texture. Generally, the second phase is divided into two groups base on their hardness:

- 1. Hard particles with hardness of 4-30Gpathat includes SiC, TiC, TiN.
- 2. Soft particles with less than 2 Gpa hardness such as Graphite, Mica and Molybdenum disulfide which acts as lubricant.

Stainless steel 304(St 304) is one of the most important austenitic stainless, due to its good formability and weldability, high corrosion and oxidation resistance, and excellent toughness at room temperature. It has numerous applications including chemical containers, food production equipment, and homogenization-sterilization devices. It is also used for making kitchen accessories, heat exchangers, and mining blades. However, it suffers from a drawback of inadequate hardness and poor wear resistance. Its poor wear resistance has an adverse impact on its performance especially when its components encounter other medium such as when turbine components experience high velocity jet leading to severe damage [15].

The objective of this study is to improve the wear performance of St 304. For this purpose, a coating of TiC is applied on the substrate. To begin with, Ti strip cored with graphite powder is made from titanium straps through drawing process. Later this wire is melted through TIG welding process to produce a composite coating on St 304.The characterization of the coating is carried out through a number of microscopic and wear resistance tests.

2. Experimental Procedures

The substrate material used in this study was St 304, the chemical composition of which is given in Table 1. Fig.1 shows the schematic of TIG coating process employed herein study.

Table 1. Chemical analysis of stainless steel (304).

Elements	Fe	Cr	Ni	C	Si	Mn	N	S	P
Percent	70.99	18.00	8.00	0.08	0.75	2.00	0.10	0.03	0.05

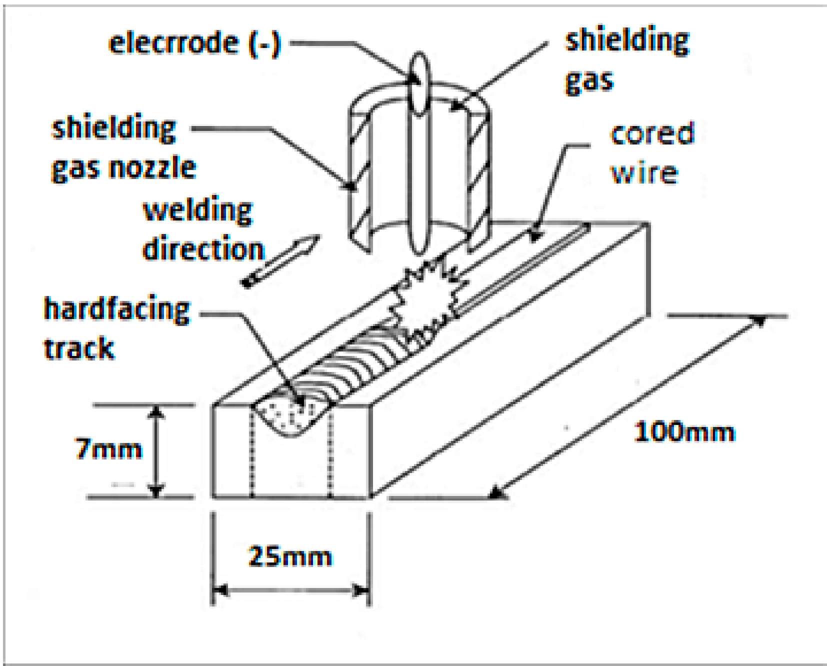

Fig.1 TIG coating process.

Ti strip cored with graphite powder was made from titanium straps through drawing process. The exit diameter of the die in the first stage of drawing was 5 mm. In the second stage of drawing, the belt was passed through a die with exit diameter of 4.1 mm. The U shape wire was passed and drawn through it, and the graphite powder was poured into a container with two holes. After passing the U shape wire through the container the belt was filled with powder and while passing through the drawing die, it was shaped as O.

The melting of this strip was done with a Tungsten electrode whose diameter was 2.4 mm. Argon flow rate was chosen as 12 L/min to protect the electrode and work piece from oxidation. The arc length used in this study was 2 mm. In this work, DCEN current polarity was selected in order to minimize electrode heating during the process. The voltage was set to 15 V. The current density and travel speed were respectively varied between 160 mA to 100 mA and 1.03 mm/min to 3.17 mm/min. A number of coating samples were produced by varying these parameters.

The coatings were sectioned perpendicular to the travel direction to prepare microstructural and mechanical samples detailed as follows. To study and calculate the element dilution in the alloying layer during coating process, samples for stereo microscopy were sectioned in thickness direction. The samples were polished and etched with Nital solution. To identify composition of the coating, SEM and X-ray analyses were done. The SEM analysis was conducted at the magnifications of 500 x and 1000 x using TESCAN Mira3. While, the X-ray diffraction was carried out by Cu Kα with current and voltage of 30 mA and 40 kV, respectively.

To investigate wear resistance of coating, the pin-on-disc test was performed. For the sake of comparison, the base metal was also subjected to wear. The pin was a cube with the dimensions of 3 × 5 × 4 mm^3 and the counter disc plate was made of cermet/cobalt/tungsten carbide with diameter of 60 mm. The hardness of the disk was about 1500 HV. The wear test was carried out for the distance of 1000 m employing a speed of 0.13 m/s and a load of 49 N. The wear was measured as weight loss of pin, which was quantified using a weighing machine within accuracy of ±0.1 mg. To study the wear mechanism, wear surfaces were examined using SEM.

Preprints (www.preprints.org) | NOT PEER-REVIEWED | Posted: 14 April 2017 doi:10.20944/preprints201704.0079.v1

Peer-reviewed version available at Coatings 2017, 7, , 80; doi:10.3390/coatings7060080

3. Discussion and Conclusion

3.1. Stereo Images

Fig. 2(a-d) show stereo images of selected samples of composite coating processed under various conditions. Some of them have inclusions. According to the cross section of welds, the dilution of the weld lines can be assessed. The amount of heat generated in TIG process is directly related to the current and voltage and inversely related to the welding speed, so with increasing the current and decreasing the speed, due to increasing in internal heat, more particles will be dissolved and as a result fewer inclusions will be formed. As an example, in the speed of 3.17 mm/s and current of 120 A, because of the small amount of heat, some inclusions were observed, therefore before dissolution of all particles, solidification has happened and these particles have remained in the sample. But in the speed of 2.1 mm/s and current of 120 A, particles have enough time to dissolve. It is due to the fact that internal heat is high and solidification time is relatively long.

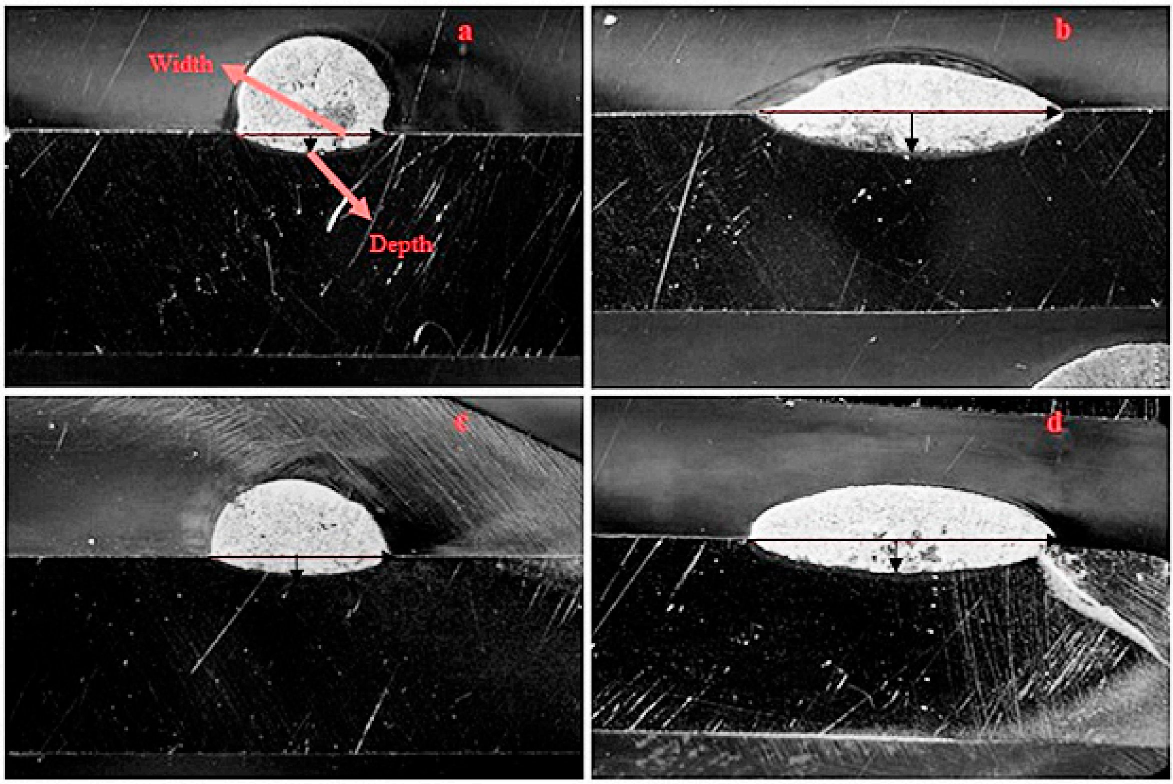

Fig 2. Stereo image of coating in a) the speed of 2.1 mm/s and current of 100 A b) the speed of 2.1 mm/s and current of 120 A c) the speed of 3.17 mm/s and current of 120 A d)the speed of 3.17 mm/s and current of 140 A.

As listed in Table 2 and can be seen in images, diffusion depth and coating width increase with increasing the current and decreasing the welding speed. The largest diffusion depth and coating width were related to the sample with the speed of 3.17 mm/s and the current of 120 A.

Table.2 Width and depth of coatings at various speeds and currents.

Speed (mm/Sec)	Current (A)	Width (mm)	Depth (mm)
2.1	120	7	0.65
3.17	120	8.1	1.6
3.17	140	**1.6**	**0.75**
2.1	110	1.65	1.1

Preprints (www.preprints.org) | NOT PEER-REVIEWED | Posted: 14 April 2017 doi:10.20944/preprints201704.0079.v1

Peer-reviewed version available at Coatings 2017, 7, , 80; doi:10.3390/coatings7060080

The dilution is the ratio of molten metal to the total amount of the molten metal during welding (sum of base metal and coating), which is usually represented as percentage. The amounts of calculated dilutions for the above images are listed in Table 3. As seen from the table, the most dilution is for the minimum speed and middle current, i.e., 2.1 mm/s and 120 A.

Table 3. The amount of dilution in various currents and speeds.

Speed (mm/Sec)	Current (A)	Dilution Amount
2.1	120	53%
3.17	120	21%
3.17	140	42%
2.1	110	17%

3.2. Microstructure and composition of coating

The below formulas explain how TiC is formed.

$$TiC \rightarrow Ti + C \quad (1)$$

$$C_{matrix} + C_{graphite} \rightarrow 2C \quad (2)$$

$$Ti + 2C \rightarrow TiC + C \text{ (supersaturated TiC phase)} \quad (3)$$

The microstructure of the substrate (St 304) and coating is respectively shown in Fig. 3(a) and 3(b).The shown coated sample was produced using the speed of 3.17 mm/s and current of 120 A. A visible difference between the substrate and coated samples can be observed. There are a series of dark particles with areas of gray fragments in the matrix.

Peer-reviewed version available at *Coatings* **2017**, *7*, , 80; doi:10.3390/coatings7060080

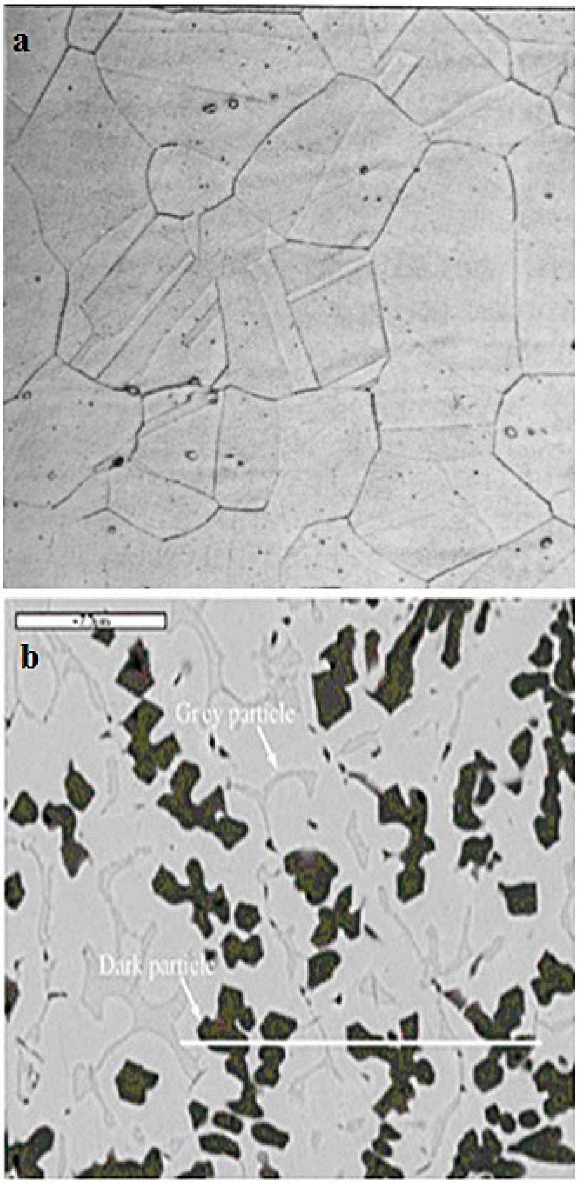

Fig.3 Microstructure of a) stainless steel in 500x and b) Composite coating microstructure in the speed of 3.17 mm/s and current of 120 A (1000x).

Fig.4 presents the chemical analysis of these black particles carried out with EPMA (Electron Probe Micro Analyzer). As can be seen, the dark particles contain carbon, titanium and a small amount of chromium: the presence of chromium in the coating is due to its high content in St 304. It seems that the black segments are the mixtures of titanium and chromium carbides. A series of fine dark areas that have been spread across the coating, and are rich in carbon and titanium can also be seen in the image. These are in fact super saturated titanium carbide [23].

$$TiC \rightarrow Ti + C \quad (4)$$

$$C_{matrix} + C_{graphite} \rightarrow 2C \quad (5)$$

$$Ti + 2C \rightarrow TiC + C \text{ (supersaturated TiC phase)} \quad (6)$$

During coating operation, the flux cored wire and some amount of the substrate melt. Through solidification process, titanium carbide and chromium carbide particles (dark areas) are formed, then

Preprints (www.preprints.org) | NOT PEER-REVIEWED | Posted: 14 April 2017 doi:10.20944/preprints201704.0079.v1

Peer-reviewed version available at Coatings 2017, 7, , 80; doi:10.3390/coatings7060080

the liquid phase transforms to the super saturated titanium carbide (fine dark particles), and iron carbide (gray fragments) that were distributed in the background γ phase [24].

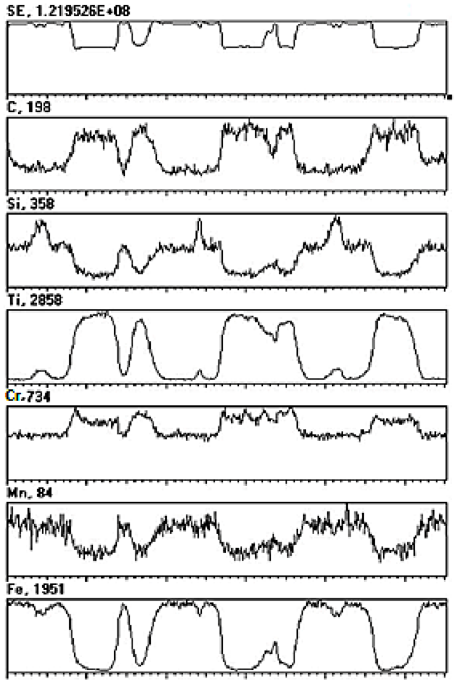

Fig 4. EPMA test results of the coating in the speed of 3.17 mm/s and current of 120.

Fig.5 shows the XRD analysis of coating. The main phases of composite coating, except the main phase, include iron carbide, titanium carbide and chromium carbide, as seen from the formulas. These results endorse the above finding that the coating contains hard particles of titanium carbide and chromium carbide.

$$TiC \rightarrow Ti + C \quad (7)$$

$$C_{matrix} + C_{graphite} \rightarrow 2C \quad (8)$$

$$3Fe + 2C \rightarrow Fe_3C + C \quad (9)$$

$$23Cr + 6C \rightarrow Cr_{23}C_6 \quad (10)$$

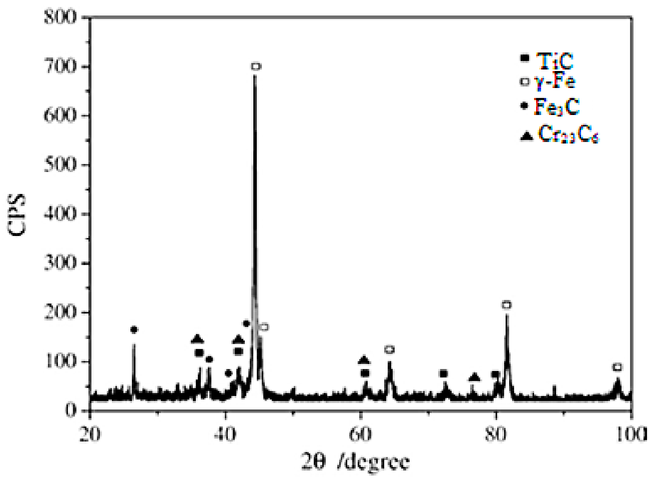

Fig.5 X-Ray diffraction of coating in the speed of 3.17 mm/s and current of 120 A.

Peer-reviewed version available at Coatings 2017, 7, , 80; doi:10.3390/coatings7060080

3.3. Micro-hardness

3.3.1. Variation of microhardness with current density

The variation of micro hardness with variation in the current density is portrayed in Fig. 6(a). As it is clear, by increasing the current density, the hardness of coating reduces since both the dilution rate and consequently the amount and volume of TiC and Cr23C6 decrease [11, 25]. In each of the given profile, the hardness initially increases from surface to substrate and then gradually decreases. It is worth noticing that the increase in the coating hardness varies from 2.5 times to 5.5 times compared to that of substrate, which can be reasoned to the formation of TiC and Cr23C6, as can be seen from Figs. 4 and 5. This value is around two times more than maximum hardness achieved by TiC layer deposited on 304St.St by means of laser beam implantation. Moreover, in this work the maximum hardness of produced alloying layer is higher compared with the maximum hardness of the coating deposited by TIG using Ferro-molybdenum and Ferro-Chromium on the surface of Austempered formable steel which is 895 HV [27].

Though the trend of hardness across the coating thickness is similar for all current densities, the variation in hardness across the thickness is different. For instance, the hardness trend corresponding to 0.8 mm thickness shows increase in hardness when the current is 120 A while the hardness shows downward trend when current is 140 A. This discrepancy can be attributed to variation in the composition of coating.

3.3.2. Variation in in micro hardness with travel speed

Change in micro hardness with change in the welding speed is shown for a number of samples in Fig. 6(b). As can be observed, the increase in the welding speed causes increase in the micro hardness. This may be attributed to dilution reduction that leads to enhancement in the amount and volume of TiC/Cr23C6 and consequently improvement in the hardness. The surface hardness of coating increases by about 80% when the speed increases from 1.03 mm/sec to 3.17 mm/sec. Thus, the trend of increasing speed is opposite to that observed for increasing current. Similar to trend found above, the hardness across coating thickness in this case also does not follow any particular trend. This type of hardness pattern has been reported for other materials as well. For instance, WC coating deposited on 4340 steel via TIG process [26]. A similar trend was also exhibited by hard coatings prepared by MIG and spraying processes on St 52 substrate [19]. Irregularity in size of second phase particles and morphology has been reported as the main reason of such trends.

Preprints (www.preprints.org) | NOT PEER-REVIEWED | Posted: 14 April 2017 doi:10.20944/preprints201704.0079.v1

Peer-reviewed version available at Coatings 2017, 7, , 80; doi:10.3390/coatings7060080

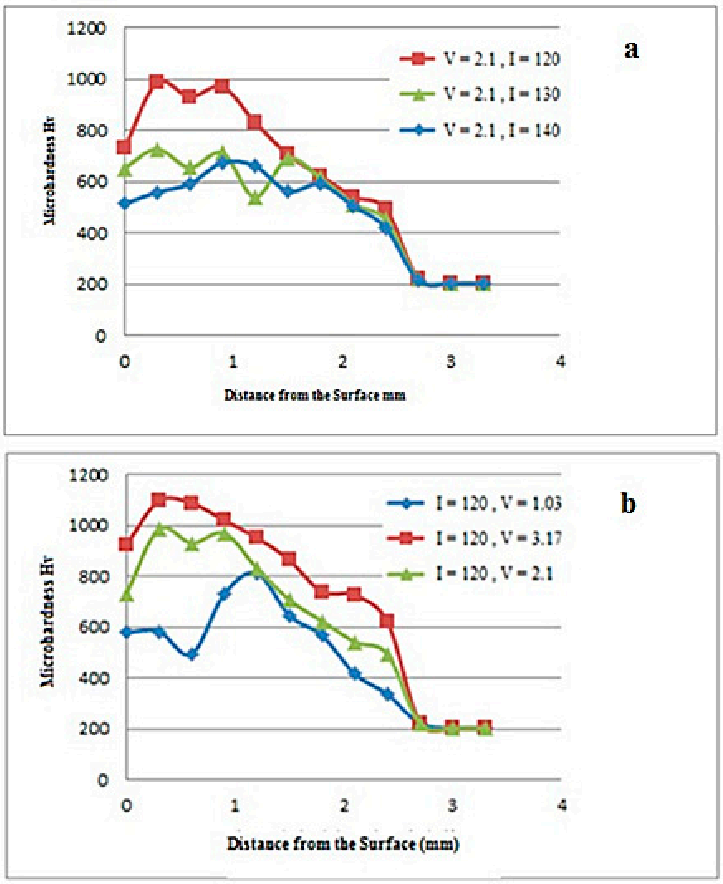

Fig 6 Changes in micro hardness based on the distance from the surface a) in a constant transmission speed and different current and b) in a constant current of 120A and different travel speeds

3.4. Wear

Fig.7 compares the amount of mass reduction in the base metal and composite coating produced with 120 A current and 3.17 mm/s travel speed. In the beginning, the difference in the wear of two samples is not significant; however, the wear of base metal visibly increases with time. For the distance of 1000 mm, the coating experiences 4.5 times (or 450%) more wear than the base metal does. Obviously, the high wear performance of coating is due to presence of hard particles TiC.

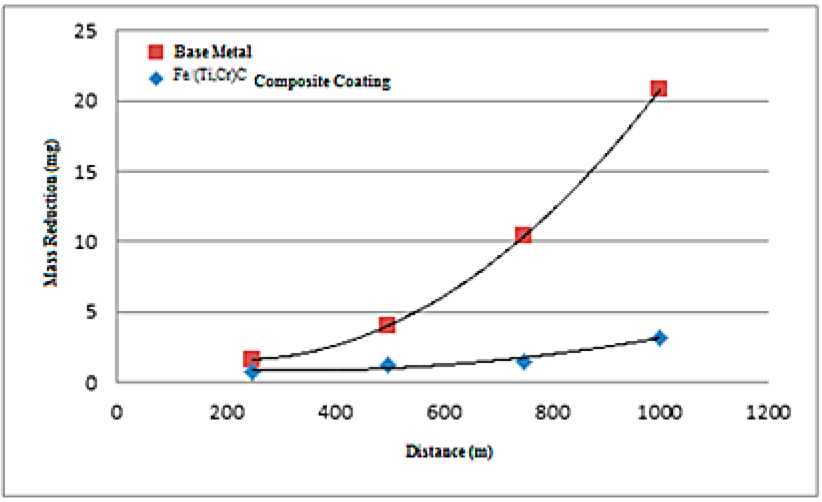

Fig. 7 Mass reduction diagram for St.St. on sample with and without composite coating.

Preprints (www.preprints.org) | NOT PEER-REVIEWED | Posted: 14 April 2017 doi:10.20944/preprints201704.0079.v1

Peer-reviewed version available at *Coatings* **2017**, *7*, , 80; doi:10.3390/coatings7060080

Fig.8 presents the friction behavior of substrate and coating. As can be seen, both substrate and coating show consistent friction behavior over distance. However, the friction co-efficient of coating is about 1.6 times smaller (or 37%) than that of the substrate. Again the better performance of coating is due to containing hard particles TiC/Cr23C6 mixture, based on the results of Fig. 4 and 5. These hard phases act as lubricant and reduce the friction between the two surfaces.

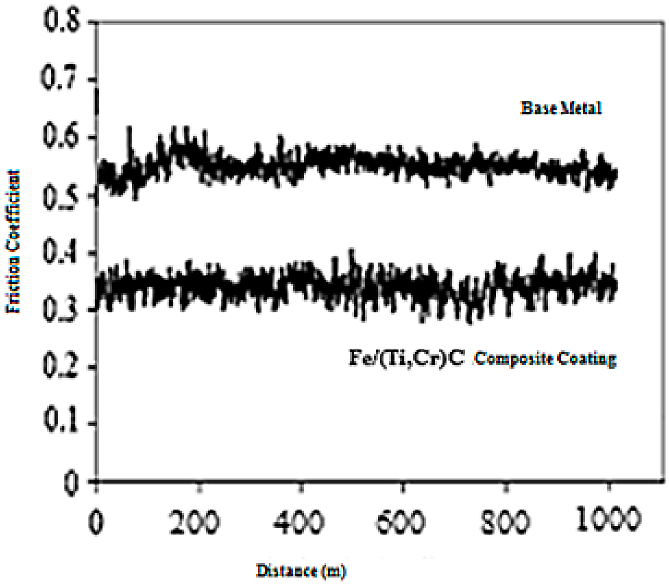

Fig. 8 Friction coefficient changes diagram based on the distance from surface for 304St.St. with and without composite coating produced in 120A current and 3.17 mm/s travel speed.

Fig.9 (a and b) show the morphology of the worn surfaces of base metal and coating. There is intensive plastic deformation, and long and parallel lines on the surface which imply the occurrence of abrasive wear in the specimen. On the other hand, coated sample contains shorter lines indicating low abrasive wear. Moreover, the sticking marks can be seen on the surface which is an indication of adhesive wear highlighting that better wear performance of coating is due to adhesion mechanism.

Preprints (www.preprints.org) | NOT PEER-REVIEWED | Posted: 14 April 2017 doi:10.20944/preprints201704.0079.v1

Peer-reviewed version available at *Coatings* **2017**, *7*, , 80; doi:10.3390/coatings7060080

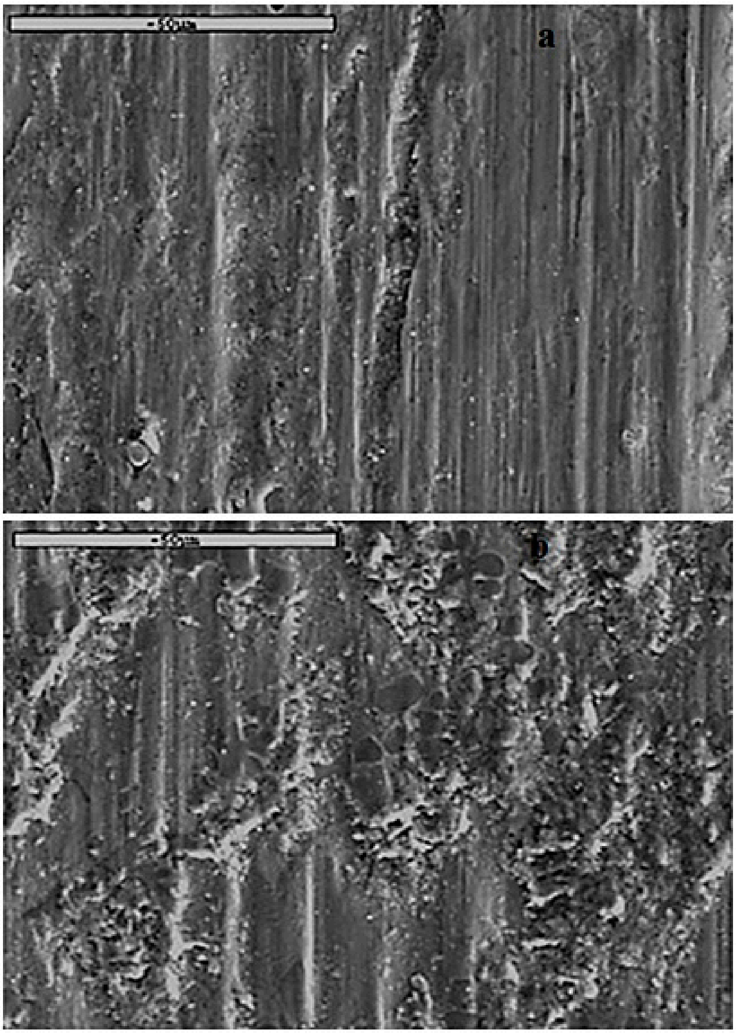

Fig.9 Wear surface of a)St.St. sample without coating layer and b)St.St. sample including (Ti,Cr)C coating layer.

4. Conclusions

This study employed TIG as a cost effective method to develop a composite coating on St 304 substrate. Ti wire cored with graphite was used to realize the desired coating. The effect of variation in the current density and travel speed was examined on the coating properties. The important results of the study are as follows:

- 1. The coating is mainly composed of TiC/Cr23C6/Fe. The microstructure of composite layer includes TiC and Cr23C6 particles besides traces of Fe3C in austenitic matrix.
- 2. Specimens coated with composite layer have more hardness than the substrate. The coating hardness can be up to1100 HV being almost 4.5 times higher than the hardness of St 304. The hardness of the deposited layer decreases by increasing the welding current density in a constant travel speed and by reducing the travel speed in a constant current density as a result of dilution rate increase and decline in the amount and volume of TiC/Cr23C6 particles in coating.
- 3. Formation of TiC/Cr23C6 hard phase in coating layer is the main reason for hardness and wear resistance enhancement and friction coefficient reduction compared with the substrate.
- 4. Friction coefficient of the optimum coating layer is around 0.35 which is about half of that of substrate (0.56).
- 5. The optimum parameters for coating are: 120 A current and 3.17 mm/s travel speed.

References

1. Handbook, A., Properties and selection: irons, steels, and high performance alloys. ASM international, 1990. 1: p. 140-194.
2. Peckner, D. and I.M. Bernstein, Handbook of stainless steels. 1977: McGraw-Hill New York, NY.
3. Sedriks, A.J., Corrosion of stainless steel, 2. 1996.
4. Kim, C.S., Thermophysical properties of stainless steels. 1975, Argonne National Lab., Ill.(USA).
5. Zotova, E., Mechanical properties of stainless steels. Metal Science and Heat Treatment, 1964. 5(7): p. 371-373.
6. Olsson, C.-O. and D. Landolt, Passive films on stainless steels—chemistry, structure and growth. Electrochimica acta, 2003. 48(9): p. 1093-1104.
7. Conrad, J.R., et al., Plasma source ion-implantation technique for surface modification of materials. Journal of Applied Physics, 1987. 62(11): p. 4591-4596.
8. Liang, W., Surface modification of AISI 304 austenitic stainless steel by plasma nitriding. Applied Surface Science, 2003. 211(1): p. 308-314.
9. Mansfeld, F., et al., Surface modification of stainless steels: green technology for corrosion protection. Surface and coatings technology, 1997. 90(3): p. 224-228.
10. Trtica, M.S., et al., Surface modification of stainless steels by TEA CO 2 laser. Applied surface science, 2001. 177(1): p. 48-57.
11. Hajbagheri, F.A., S.K. Bozorg, and A. Amadeh, Microstructure and wear assessment of TIG surface alloying of CP-titanium with silicon. Journal of Materials Science, 2008. 43(17): p. 5720-5727.
12. Kwok, C., F. Cheng, and H. Man, Laser surface modification of UNS S31603 stainless steel using NiCrSiB alloy for enhancing cavitation erosion resistance. Surface and Coatings Technology, 1998. 107(1): p. 31-40.
13. Proskurovsky, D., et al., Pulsed electron-beam technology for surface modification of metallic materials. Journal of Vacuum Science & Technology A, 1998. 16(4): p. 2480-2488.
14. Hao, S., et al., Microstructure evolution occurring in the modified surface of 316L stainless steel under high current pulsed electron beam treatment. Applied surface science, 2007. 253(12): p. 5349-5354.
15. Buytoz, S. and M. Ulutan, In situ synthesis of SiC reinforced MMC surface on AISI 304 stainless steel by TIG surface alloying. Surface and Coatings Technology, 2006. 200(12): p. 3698-3704.
16. Liu, S.-G., et al., High temperature erosion properties of arc-sprayed coatings using various cored wires containing Ti–Al intermetallics. Wear, 2007. 262(5): p. 555-561.
17. Yang, K., et al., Effect of carbonitride precipitates on the abrasive wear behaviour of hardfacing alloy. Applied Surface Science, 2008. 254(16): p. 5023-5027.
18. Klimpel, A., et al., The study of properties of Ni–WC wires surfaced deposits. Journal of materials processing technology, 2005. 164: p. 1046-1055.
19. Amushahi, M., F. Ashrafizadeh, and M. Shamanian, Characterization of boride-rich hardfacing on carbon steel by arc spray and GMAW processes. Surface and Coatings Technology, 2010. 204(16): p. 2723-2728.
20. Chatterjee, S. and T. Pal, Wear behaviour of hardfacing deposits on cast iron. Wear, 2003. 255(1): p. 417-425.
21. Watanabe, T., T. Sato, and A. Nezu, Electrode phenomena investigation of wire arc spraying for preparation of Ti-Al intermetallic compounds. Thin Solid Films, 2002. 407(1): p. 98-103.
22. Chang, C.-M., et al., Microstructure and wear characteristics of hypereutectic Fe–Cr–C cladding with various carbon contents. Surface and Coatings Technology, 2010. 205(2): p. 245-250.
23. Zhang, S.H., et al., Characterization on the coatings of Ni-base alloy with nano-and micron-size Sm 2 O 3 addition prepared by laser deposition. Materials Chemistry and Physics, 2008. 112(2): p. 668-674.
24. Xinhong, W., et al., Microstructure and wear properties of in situ TiC/FeCrBSi composite coating prepared by gas tungsten arc welding. Wear, 2006. 260(1): p. 25-29.

25. Wang, X., et al., Fabricating TiC particles reinforced Fe-based composite coatings produced by GTAW multi-layers melting process. Materials Science and Engineering: A, 2006. 441(1): p. 60-67.
26. Buytoz, S., M. Ulutan, and M.M. Yildirim, Dry sliding wear behavior of TIG welding clad WC composite coatings. Applied Surface Science, 2005. 252(5): p. 1313-1323.

27. A. Amirsadeghi, M. Heydarzadeh Sohi, Comparison of the influence of molybdenum and chromium TIG surface alloying on the microstructure, hardness and wear resistance of ADI, Journal of Materials Processing Technology, 2008, Pages 673–677.